Sigma J Eng & Nat Sci 37 (4), 2019, 1181-1198

Sigma Journal of Engineering and Natural Sciences
Sigma Mühendislik ve Fen Bilimleri Dergisi

Research Article

VIBRATIONAL ANALYSIS AND HYDROGEN-BONDING EFFECTS ON THE VIBRATIONAL MODES OF ZWITTERIONIC DL-TRYPTOPHAN: IR SPECTROSCOPY AND DFT CALCULATIONS

Abdelali BOUKAOUD*[1], Younes CHIBA[2], Mourad DEHBAOUI[3], Nacir GUECHI[4]

[1]*Laboratoire de Physique des Techniques Expérimentales et ses Applications, Université de Médéa, ALGERIA;* ORCID: 0000-0003-2190-9152
[2]*Department of Mechanical Engineering, Faculty of Science and Technology, University of Medea, ALGERIA;* ORCID: 0000-0003-0560-5212
[3]*Laboratoire de Physique des Techniques Expérimentales et ses Applications, Université de Médéa, ALGERIA;* ORCID: 0000-0001-8681-5099
[4]*Laboratoire d'Etudes des Surfaces et Interfaces des Matériaux Solides, University Ferhat Abbas Setif 1, Setif 19000, ALGERIA;* ORCID: 0000-0001-9328-8362

Received: 15.04.2019 Revised: 07.06.2019 Accepted: 24.07.2019

ABSTRACT

The vibrational behavior of zwitterionic DL-tryptophan has been investigated using infra-red spectroscopy and density functional theory calculations. In order to study the hydrogen bonding effects on the molecular structure and vibrational normal modes of the under-investigated amino acid, both the solid state and aqueous solution calculations have been presented. The three dimensional molecular structure optimized by the solid state calculations shows the best agreement with that previously published using X-Ray diffraction technique. In addition, the calculated and experimentally observed wavenumbers have been compared. However, only the calculations performed in the solid state allowed us to attribute the band observed at around 2532 cm^{-1} to the N-H stretching vibration. Because some normal modes are strongly affected by the extensive hydrogen bonding network present in DL-tryptophan crystal, the solid state model is the most suitable for interpreting the experimental infra-red spectrum.
Keywords: DL-tryptophan, amino acids, IR spectroscopy, DFT calculations.

1. INTRODUCTION

Amino acids are the main building blocks of proteins, they play a very important role in almost all the biological mechanisms in Nature. The molecular structures of amino acids have both carboxyl and amino groups as substituents on the same carbon atom called α-carbon. However, the amino acids with both positive (NH^+_3) and negative (COO^-) electrical charges are known as zwitterionic amino acids [1]. With the exception of glycin, amino acids can exist in two enantiomeric forms: L or D-forms. A mixture of equal amounts of the two forms of amino acids is called a racemic compound (DL-form) [2].

* Corresponding Author: e-mail: boukaoud.abdelali@univ-medea.dz, tel: +213(0) 55 32 66 943

The ability to distin guish between the L, D and DL-forms of amino acids is naturally manifested in our biological world. It has been shown that "almost" only the L-form is naturally present in proteins [3]. In fact, this intimate property of our biological World remains a mystery and its origin is still unknown until now [4,5].

Since the early 20th century, tryptophan has been the subject of intensive spectroscopic studies [6]. Some of them showed that the ability of proteins to absorb the UV radiations is mainly due to the presence of amino acids, and tryptophan has the strongest absorption near 280 nm [7]. The IR spectra of L-tryptophan were reported by several researchers [8,9]. However, the detailed vibrational analysis was performed by X. Cao et al. [10].

From a crystallographic point of view, it has been experimentally confirmed that the crystal structures of DL-tryptophan [11,12] and L-tryptophan [13] are completely different, they crystallize in the monoclinic (space group $P2_1/c$) and triclinic (space group P1) systems, respectively. Recent studies have also revealed changes in the spectroscopic behavior of many L- and DL-forms of amino acids, such as: L- and DL-histidine [14], L- and DL-alanine [15] and L- and DL-serine [16,17]. All these studies showed that the differences between the vibrational spectra of L-and DL-amino acids are mainly caused by the peculiarities of their inter-molecular interactions. It is important to note that each amino acid crystal has its specific hydrogen bond (H-bond) network, which plays a major role in determining the most stable molecular conformation. Theoretically, the inclusion of solvation effects in the calculations for predicting the most stable molecular conformations of amino acids have been widely employed. However, such approaches can encounter two difficulties: (i) the first one, is the large number of possible conformers which characterizes the amino acid molecules [18,19], (ii) the second difficulty is that the effects of inter-molecular interactions which appear, in general, in the region higher than ~1600 cm^{-1} in the experimental IR spectra of amino acids (KBr pellet techniques) [10,20,21] cannot be correctly taken into account in the calculations.

Experimentally, several methods based on the matrix isolated monomeric molecules of amino acids have been developed to improve the agreements between the observed and calculated IR spectra [10]. However, such methods eliminate the “real effects” of inter-molecular interactions which can be differentiated the IR spectra of L, D-and DL-amino acids.

In our study, the IR spectrum recorded in the solid phase has been studied to reveal the effects of inter-molecular interactions on the vibrational modes of the considered compound, and the periodic (solid state) calculations have been employed to overcome the problems of molecular conformations and inter-molecular interactions.

The main aim of this work is to better understand the effects of hydrogen bonding on the structural and vibrational normal modes of DL-tryptophan. To this end, its molecular structure has been predicted in both solution and the solid state and compared with previously reported experimental results. Also, for the first time, the IR spectrum of DL-tryptophan, recorded in the region 600–4000 cm^{-1}, has been fully studied employing non-periodic and periodic calculations.

2. MATERIALS AND METHODS

2.1. Experimental details

The zwitterionic form of DL-tryptophan (≥ 99%) was supplied by Sigma Aldrich and utilized without further purification.

At room temperature, the FT-IR spectrum of powder of DL-tryptophan was recorded in the region 600–4000 cm^{-1} using solid-state sample, on a JASCO FT/IR-6300 spectrometer. The spectral resolution of the spectrometer was 4 cm^{-1}.

2.2. Computational details

For the aqueous-solution model, DFT calculations were carried out with the ORCA 3.0.3 program [22], with the use of water as solvent. The initial geometry of DL-tryptophan was generated without any constraints from single crystal X-ray diffraction results [12]. The optimized geometrical parameters, vibrational wavenumbers and IR intensities were calculated by using the hybrid DFT method B3LYP [23,24], the def2-TZVP basis set [25,26] and also the def2-TZVP/J auxiliary basis set. In these calculations, the concerning energy terms were obtained by using the RIJCOSX algorithm [27,28]. The systematic errors due to the neglect of the anharmonic effects were compensated by using the correlation expression below, which is similar to those proposed by Osaki and Soejima [29] and Yoshida et al. [30].

$$\omega_{scal} = -0.000028\ \omega^2_{cal} + 1.034\ \omega_{cal} - 14.77 \quad (cm^{-1}) \tag{1}$$

Here, ω_{scal} and ω_{cal} are the scaled and calculated wavenumbers for each vibrational mode, respectively.

The solid phase calculations for DL-tryptophan in crystal structure were realized in the GGA (generalized-gradient-approximation) by using the PBE (Perdew–Burke–Ernzerhof) functional [31] in the CASTEP program [32]. In the calculations, the norm-conserving pseudopotentials and the plane-wave cut-off energy of 830 eV were employed. Brillouin zone sampling of electronic states was performed on 1 × 2 × 2 Monkhorst Pack grids. The harmonic vibrational wavenumbers were obtained by using the optimized structure and employing the linear response method within the density functional perturbation theory (DFPT) [33] at the Gamma point.

3. RESULTS AND DISCUSSION

3.1. Geometry optimization

The optimized molecular structure of DL-tryptophan in aqueous solution is shown in Figure 1a. Figures 1b and 1c represent the optimized unit cell and the molecular packing restricted by inter-molecular N-H···O H-bonds in the solid phase, respectively. The observed (X-Ray) [12] and computed unit-cell parameters are listed in Table I.

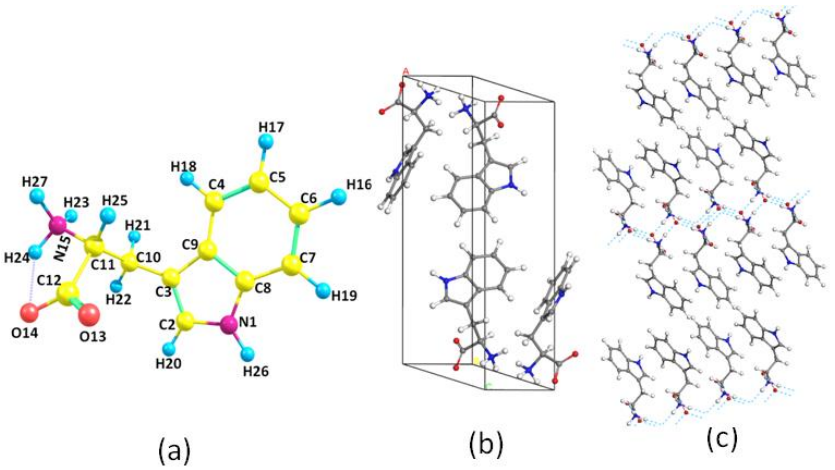

Figure 1. The optimized geometries obtained at the Density Functional Theory approach for the molecular and crystal structures of DL-tryptophan. (a) the optimized molecular structure obtained by the aqueous solution model; (b) the optimized geometry obtained for the unit cell of DL-tryptophan by using the solid phase model; (c) the molecular packing obtained by using the solid phase model.

Table 1. A comparison between the calculated and experimentally measured unit cell parameters obtained for DL-tryptophan crystal.

Unit cell parameters	Calculated (a)	Experimental (b)
a (Å)	18.9602	18.899(2)
b (Å)	5.7709	5.7445(6)
c (Å)	9.1280	9.309(1)
β(°)	100.956	101.776(2)
V ($Å^3$)	980.56	989.4(4)

(a) The modelled unit cell is shown in Figure 1b.
(b) The experimental unit cell parameters were taken from ref. [12].

Our results show that the calculated unit-cell parameters are in good agreement with the ones obtained by using X-ray diffraction ; the unit-cell volume calculated with the PBE method is about 0.9 % less than the experimentally observed one.

As can be seen in Figure 1c, the NH^+_3 group forms three intermolecular N-H···O H-bonds with carboxyl oxygen atoms of adjacent molecules, the computed distances between donor and acceptor atoms are ranging from 2.684 to 2.821Å. It is important to mention that the stability of DL-tryptophan in the solid state is strongly dependent on this extensive network of H-bonds. Therefore, significant differences between the computed dihedral angles in aqueous solution and the corresponding ones obtained experimentally can be expected.

Some selected optimized geometry parameters of DL-tryptophan molecule (bond lengths, bond angles and dihedral angles) are listed in Table II in comparison with the corresponding experimental parameters [12]. The numbering scheme used for the atoms in the table is as given in Figure 1a.

Table 2. A comparison between the calculated and experimentally measured geometry parameters obtained for DL-tryptophan molecule.

Bond lengths (Å)			
Parameters (a)	Solution phase model (b)	Solid phase model (c)	Experimental [12]
N1C2	1.373	1.372	1.373(2)
C2C3	1.3701	1.376	1.359(2)
C3C9	1.4393	1.439	1.435(2)
C3C10	1.4957	1.484	1.490(1)
C4C5	1.3861	1.393	1.375(2)
C4C9	1.4034	1.402	1.393(2)
C5C6	1.4076	1.410	1.397(2)
C6C7	1.3866	1.390	1.374(2)
C7C8	1.3955	1.399	1.391(2)
C8C9	1.4213	1.428	1.414(1)
C10C11	1.5428	1.546	1.537(1)
C11N15	1.5042	1.456	1.486(1)
C11C12	1.5544	1.534	1.522(1)
C12O14	1.2601	1.270	1.263(1)
C12O13	1.2423	1.2	1.238(1)
Bond angles (°)			
C3 C3C10C11	115.048	114.84	113.71(8)
N15C11C12	106.370	110.12	109.50(8)
N15C11C10	108.352	109.84	109.61(8)
C12C11C10	112.521	111.14	112.16(8)
O13C12O14	128.215	126.11	125.95(9)
O13C12C11	116.738	119.25	117.60(8)
O14C12C11	115.033	114.63	116.45(9)
Dihedral angles (°)			
C2C3C10C11	107.59	104.00	107.9(1)
C3C10C11N15	171.88	163.3	166.78(8)
C3C10C11C12	-70.79	-74.57	-71.4(1)
N15C11C12O13	-155.30	-157.90	-158.0(1)
N15C11C12O14	25.95	22.29	21.7(1)
C10C11C12O14	-92.53	-99.65	-100.3(1)

(a) The atom numbering scheme is given in Figure 1a.
(b) The calculation model used for the aqueous solution phase of DL-tryptophan.
(c) The calculation model used for DL-tryptophan in solid phase.

It can be seen from Table II that the computed bond lengths for both solution and solid phase models are almost in good agreement with the observed results, the main deviation between them is found to be 0.03 Å for the C11-C12 bond length.

The same observation holds true for the bond angles, where the root mean square (rms) deviation between the predicted and observed bond angles are about 1.74° (solution model) and 1.12° (solid phase model).

In contrast, the calculated C10-C11-C12-O14 dihedral angle at -92.53° in aqueous solution and experimentally observed at -100.3(1)° is the most affected by the H-bonding network. This difference (~7.77°) is due to the effect of the intra-molecular N15H24··· O14 H-bond (Figure 1a), noting that this H-bond is missing in the crystal of DL-tryptophan [12]. In the solid state model, this difference is reduced to 0.6°. On the other hand, the differences found between the computed (aqueous solution model) and the observed N15-C11-C12-O13 and N15-C11-C12-

O14 dihedral angles are 2.7° and 3.6°, respectively. These differences are attributed, as expected above, to the effects of inter-molecular (H-bonds) interactions which are not correctly taken into account in the solution-phase calculations.

With only a few exceptions, such as the C2-C-3C10-C11 and C3-C10-C11-C12 dihedral angles, it can be concluded that the computed geometrical parameters using the solid state calculations show the best agreement with the observed molecular structure.

3.2. Vibrational analysis

In this section, in which the assignments of the vibrational bands observed in the FT-IR spectrum of DL-tryptophan are presented and evaluated, a comparison of the experimental results with those previously reported for L-tryptophan is given and the simulated IR spectra for the title compound in solution and in solid phase circumstances are presented; please see Figure 2 for the recorded experimental FT-IR spectrum of DL-tryptophan.

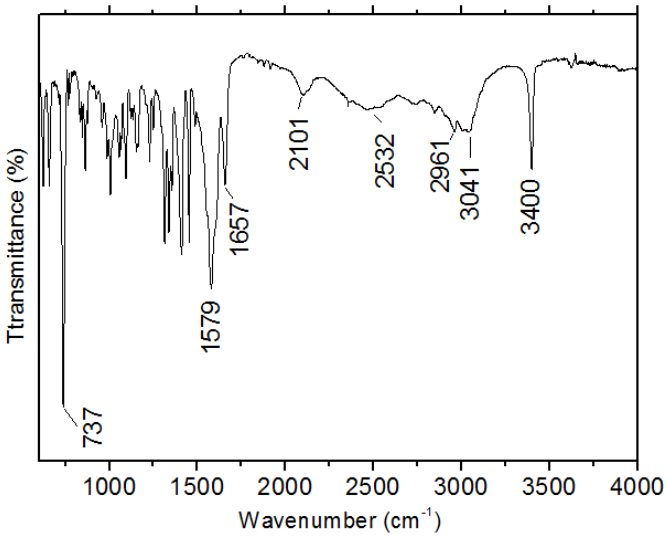

Figure 2. The experimental IR spectrum of DL-tryptophan

As a first observation, the FT-IR spectra recorded for the DL-tryptophan (Figure 2) and L-tryptophan (KBr disc technique)[10] are similar to each other, but not exactly identical. As the band intensities are considered, it is seen that the strongest band in the FT-IR spectrum of DL-tryptophan is centered at 737 cm^{-1}, while the strongest three bands observed in the IR spectrum of L-tryptophan, which have almost the same intensity, are centered at 744, 1590 and 3402 cm^{-1}.

It is important to note that there is a general tendency of down-shifting (or red-shifting) for the positions of the bands observed in the FT-IR spectrum of DL-tryptophan in comparison to the corresponding IR bands observed for L-tryptophan. However, the IR band observed at 2100 cm^{-1} (for L-tryptophan, the IR band at 2073 cm^{-1}) is an exception for this situation.

Moreover, it is remarkable that the region between 1657 and 2845 cm^{-1} in the observed FT-IR spectrum of DL-tryptophan, is characterised by some broad-bands. This region is similar to those observed for the majority of IR spectra of amino acids, they almost all have a particular band at around 2100 cm^{-1} [10,19-21,34]. However, an assertive interpretation of the origin of this band has not yet been given, for example; the observed band at 2040 cm^{-1} in the IR spectrum of

L-serine was assigned to the combined vibration δNH^{+}_{3} and τNH^{+}_{3} [16], the band observed at 1991 cm^{-1} for L-histidine perchlorate [35] was attributed to the overtones and combinational tones, moreover, a similar band was appeared at 2073 cm^{-1} for L-tryptophan (KBr pellet method), but it was not observed in the spectrum recorded by using the dissolution-spray-deposition (DSD) technique [10].

In the following, the calculated IR spectra using both the solid state and aqueous solution models will be presented and analyzed to get better understanding of the vibrational behavior of DL-tryptophan.

The DL-tryptophan molecule belongs to C_1 symmetry point group, it has 27 atoms, which gives 3n - 6 = 75 normal modes of vibration (n is the number of atoms in the molecule). The aqueous solution computations give the harmonic vibrational wavenumbers of the 75 internal modes as they are given in Appendix **A**. In order to obtain a good agreement between the calculated and observed wavenumbers, the correlation relation given by the equation (1) was used. Figure 3 shows the quadratic regression plot between the experimental and theoretical wavenumbers which is fitted into a quadratic equation. The theoretical IR spectrum obtained in the aqueous solution model, which is shown in Figure 4a, was produced over the harmonic wavenumbers fitted by using this correlation relation.

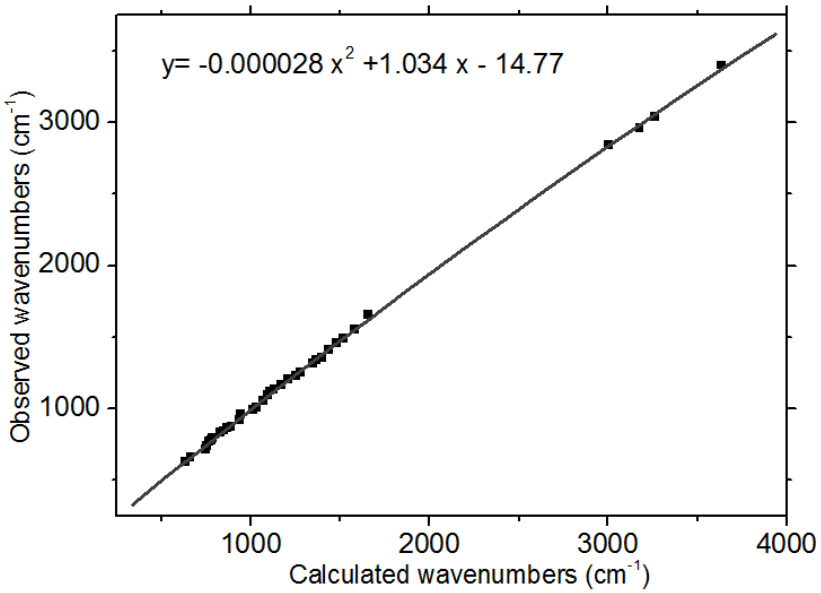

Figure 3. The correlation between the calculated and observed wavenumbers for DL-tryptophan molecule.

For the solid phase calculations, the unit cell contains four molecules (108 atoms), each atom has three degrees of freedom, therefore there are 324 modes distributed between internal modes, lattice modes, librational modes and three acoustic modes. The acoustic modes are computed as small values close to zero at -0.063, -0.051 and -0.037 cm^{-1}, the remaining 321 optical modes are classified, according to the irreducible representation of the C_{2h} factor group, into four subgroups a_g, b_g, a_u and b_u as can be seen in Appendix B. Where: a_u and b_u are the IR active modes, and a_g and b_g are the RAMAN active modes [36]. In our case, the irreducible representations of the optical modes are given as: $\Gamma_{Optical} = 81a_g + 81b_g + 80a_u + 79b_u$.

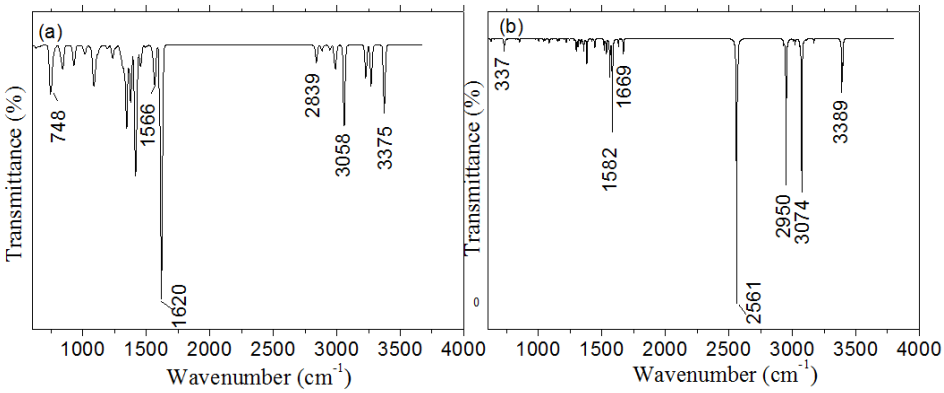

Figure 4. The infrared (IR) spectra calculated for DL-tryptophan by using the Density functional theory. (a) the scaled theoretical IR spectrum obtained by the aqueous solution model; (b) the theoretical IR spectrum obtained by the solid-state model.

The observed and calculated wavenumbers in the region 600-4000 cm^{-1} with their assignments are listed in Table III.

Table 3. A comparison between the experimental and calculated wavenumbers obtained for DL-tryptophan.

ω(obs) (a)	Solution model (b)			Solid phase model (c)				
	ω(calc)	ω(scal)	Assignment	a_g modes	b_g modes	a_u modes	b_u modes	Assignment
3400	3636 (204)	3375 (204)	ν N_1H_{26}	3389 (00)	3396 (00)	3397 (1163)	3389 (2039)	ν N_1H_{26}
3041	3260 (245)	3058 (245)	ν $N_{15}H$	3045 (00)	3079 (00)	3057 (181)	3074 (6062)	ν $N_{15}H$
2961	3176 (48)	2987 (48)	ν CH	2933 (00)	2935 (00)	2965 (7)	2950 (5782)	νs $N_{15}H$
2845	3004 (54)	2839 (54)	νs CH_2	2930 (00)	2931 (00)	2932 (86)	2932 (93)	νs CH_2
2532				2559 (00)	2557 (00)	2561 (10422)	2571 (868)	ν $N_{15}H$
2101								γ NH_3^+ + τ NH_3^+
1657	1655 (700)	1620 (700)	ν_{as} $-COO^-$	1656 (00)	1643 (00)	1650 (11)	1669 (620)	γas NH^+_3
1579	1598 (119)	1566 (119)	γ NH^+_3	1562 (00)	1565 (00)	1562 (1443)	1582 (3655)	γas NH^+_3, ν $-COO^-$
1553	1581 (17)	1550 (17)	β CH (ring), νC_2C_3	1557 (00)	1560 (00)	1558 (36)	1559 (2)	β CH (ring)
1487	1520 (6)	1492 (6)	β CH (ring)	1479 (00)	1471 (00)	1474 (10)	1475 (12)	β CH (ring), ν $-COO^-$
1455	1481 (46)	1455 (46)	β CH (ring), β $H_{21}C_{10}H_{22}$	1444 (00)	1442 (00)	1443 (170)	1445 (179)	β CH (ring), β CH_2
1409	1439 (357)	1415 (357)	γ NH^+_3	1418 (00)	1424 (00)	1423 (2)	1419 (98)	β NH (ring), β CH (ring)
1356	1399 (165)	1377 (165)	γCH_2, γNH	1359 (00)	1355 (00)	1355 (101)	1358 (465)	β NH (ring), β CH (ring)
1339	1365 (185)	1344 (185)	δ ring, ν CC	1330 (00)	1339 (00)	1330 (214)	1337 (10)	γCH_2
1314	1346 (40)	1326 (40)	γCH_2	1312 (00)	1311 (00)	1311 (202)	1311 (108)	γ CH_2

1249	1276 (8)	1259 (8)	β CH (ring)	1245 (00)	1243 (00)	1245 (18)	1244 (60)	β CH (ring)
1229	1250 (38)	1234 (38)	βCH (ring), βNH (ring)	1220 (00)	1222 (00)	1220 (138)	1220 (6)	γNH^{+}_{3}
1209	1209 (10)	1194 (10)	$\gamma(CH_2$, CH, NH)	1199 (00)	1199 (00)	1200 (10)	1201 (20)	γCH_2, γCH, γNH_3
1164	1174 (3)	1160 (3)	βCH (ring)	1155 (00)	1164 (00)	1151 (124)	1163 (70)	$\gamma\ NH^{+}_{3}$,
1133	1130 (25)	1118 (25)	β CH (ring), γCH, γNH	1124 (00)	1132 (00)	1122 (6)	1132 (11)	β CH (ring), γCH_2
1122	1107 (67)	1095 (67)	βCH (ring), βNH (ring)	1112 (00)	1109 (00)	1109 (10)	1112 (33)	β CH (ring)
1095	1095 (92)	1084 (92)	γNH^{+}_{3}, β CH(ring), βNH (ring)	1085 (00)	1088 (00)	1087 (95)	1083 (168)	β CH (ring), βNH (ring)
1055	1069 (6)	1059 (6)	$\gamma(NH^{+}_{3})$	1052 (00)	1056 (00)	1056 (33)	1054 (42)	γ NH^{+}_{3}, β CH (ring), βNH (ring)
1006	1029 (22)	1020 (22)	βCH (ring)	1004 (00)	1004 (00)	1004 (10)	1002 (114)	β CH (ring)
988	1016 (10)	1007 (10)	ν $C_{11}N_{15}$	970 (00)	972 (00)	979 (13)	976 (47)	$\gamma\ NH^{+}_{3}$
959	946 (10)	938 (10)	γCH (ring)	949 (00)	953 (00)	954 (1)	954 (11)	β CH_2
923	935 (24)	927 (24)	β (CH_2), γ (NH^{+}_{3})	906 (00)	914 (00)	912 (11)	919 (12)	γ CH (ring)
875	890 (2)	883 (2)	δ ring	865 (00)	866 (00)	864 (7)	867 (18)	δ ring
863	865 (1)	859 (1)	γCH (ring)	850 (00)	852 (00)	851 (144)	850 (9)	γ CH (ring)
845	847 (69)	841 (69)	γCH(ring)	839 (00)	839 (00)	841 (3)	834 (52)	γCH (ring)
835	829 (25)	823 (25)	γCH (ring), βOCO^{-}	821 (00)	820 (00)	819 (6)	820 (31)	γCH (ring)
792	786 (5)	781 (5)	Δ ring	765 (00)	762 (00)	764 (1)	762 (7)	Δ ring
778	777 (8)	772 (8)	δ ring, γOCO^{-}	757 (00)	758 (00)	760 (5)	755 (25)	Δ ring
766	767 (17)	762 (17)	γ OCO^{-}	747 (00)	747 (00)	749 (3)	746 (52)	Δ ring
737	753 (77)	748 (77)	γ CH (ring)	735 (00)	746 (00)	734 (16)	737 (191)	γCH (ring)
715	749 (70)	744 (70)	γCH (ring)	732 (00)	736 (00)	729 (321)	729 (165)	γCH (ring)
658	663 (4)	658 (4)	Δ ring, β (NH^{+}_{3})	650 (00)	649 (00)	652 (5)	649 (31)	Δ ring, γNH^{+}_{3}
625	636 (9)	631 (9)	Δ ring, γ CH (ring),γNH (ring)	629 (00)	623 (00)	622 (33)	627 (112)	γNH

(a) The fundamental bands observed in the FT-IR spectrum of DL-tryptophan.
(b) The calculation model used for the aqueous solution phase of DL-tryptophan ; ω(calc.): the harmonic wavenumbers calculated at B3LYP/def2-TZVP level of theory ; ω(scal.): the scaled harmonic wavenumbers derived from the calculated harmonic wavenumbers by using the correlation relation (see section 2.2.).
The symbols « ν » , «β» , «Δ» , «δ», « τ » and « γ » represent bond stretching, angle bending, out-of-plane deformation, in-plane deformation, torsion and out-of plane angle bending vibrations, respectively.
(c) The calculation model used for DL-tryptophan in solid phase ; the calculated wavenumbers obtained for the normal modes of "a_g", "b_g", "a_u" and "b_u" symmetry classes are listed in separate columns.
The calculated IR intensities (in parentheses) are expressed in Km/mole.

3.2.1. The 2845-3400 cm^{-1} spectral region

The strong band observed experimentally at 3400 cm^{-1} (Figure 2) is assigned to the N1H26 stretching vibration in both the solid state and aqueous-solution models, it is predicted at ~3397 cm^{-1} (solid-state model) and at 3375 cm^{-1} (aqueous-solution model). Clearly, the solid state calculations show the best agreement. The assignment of this band agrees with a previous assignment proposed by X. Coa et al. [10].

Similarly, the band observed at 3041 cm^{-1} is assigned to N15H stretching vibration in the solid and solution models, this band was previously observed at 3079 cm^{-1} for L-tryptophan [10], which makes it the most sensitive to the hydrogen bond network. The shift of 38 cm^{-1} reflects the difference in energy between the N–H···O H-bonds in L-and DL-tryptophan crystals [15]. However, the weak band observed experimentally at 2961 cm^{-1} is assigned to the indole C-H stretching vibrations (aqueous solution model), and to the $N_{15}H$ symmetric stretching vibration (solid state model). Finally, in both models the observed band at 2845 cm^{-1} is assigned to the CH_2 symmetric stretching vibration. The corresponding calculated bands by using the solution phase and solid phase models are predicted at 2839 and 2930 cm^{-1}, respectively. It is remarkable that the computed wavenumber by using the solid phase model is higher by about 91 cm^{-1} than the one calculated by using the solution phase model. This large deviation may be due to the neglect of the anharmonic effects in the calculations performed in the solid phase because all the computed wevenumbers were note scaled [36], it is important to remember here that in our study only the calculated spectrum by using the solution phase model was scaled and corrected for anharmonicity.

Previous studies performed on amino acids showed that the band observed at 2840 cm^{-1} in the IR spectrum of L-tryptophan, which was recorded by using the dissolution-spray-deposition (DSD) technique, was assigned to the CH_2 stretching mode [10]. Also, the band observed at 2829 cm^{-1} in the experimental IR spectrum of L-tyrosine (solid phase) was assigned to the CH_2 stretching mode [19]. These studies agree with the assignment proposed here for the band observed at 2845 cm^{-1}.

3.2.2. The 1658-2845 cm^{-1} spectral region

As mentioned above, the region ~1700-2700 cm^{-1} in the IR spectra of amino acids is characterized by a certain number of broad-bands. Some previous studies showed that the inclusion of solvation effects in the calculations does not lead to the prediction of absorption bands in this region [10,19-21]. Our calculated spectrum using the aqueous solution model agrees with these studies. Figure 4 shows a comparison between the calculated spectra by the solid and solution models. It is remarkable that an additional band appears at around 2561 cm^{-1} (predicted only by the solid state model) (Figure 4b). This bans is remarkably the most intense in the simulated IR spectrum (I_{ir} =10422 Km/mole). This result agrees with previous studies performed on glycine and L-alanine, where the computed IR spectra in the solid phase by using the PW91 functional showed the presence of two strongest bands at around 2651 cm^{-1} [36].

Employing the periodic DFT results, this band is assigned to the N-H stretching vibration as shown in the animation (Supplemental Material S1). The appearance of this band (Figure 4b) is not surprising, recently, A. Pawlukojc et al. [37] assigned the band observed at 2480 cm^{-1} in the IR spectrum of L-asparagine to the N-H···O stretching vibration, F. Parker et al. assigned the observed band at ~ 2545 cm^{-1} in the IR spectrum of L-cysteine to the S-H stretching vibration [38]. In addition, the computed wavenumber at 2650 cm^{-1} (solid state calculations) for Glycine was assigned to the N-H stretching vibration [36].

On the other hand, the observed band at 2101 cm^{-1} (Figure 2) has not correspondence in the calculated spectrum by the solid state model. In the most recent works on the amino acids, a similar band observed at 2084 cm^{-1} in the IR spectrum of L-asparagine was assigned to a

combination mode [37], but it was not assigned in the case of L-cysteine despite its appearance in the vibrational spectra [38].

The appearance of this band may be the consequence of the extensive H-bonding networks in amino acid crystals where the NH_3^+ group forms three H-bonds, which is in general a peculiarity of amino acid crystals [11,12,17,36,39-41]. In this study, and in accordance with previous work [16,34], this band is attributed to the combination mode of out-of -plane binding and torsion of NH^+_3 group. This mode is probably due to the effect of three N–H···O H-bonds on the NH^+_3 group as can be seen in the animation (Supplemental Material S2).

3.2.3. The region below 1657 cm^{-1}

The strong band observed at 1657 cm^{-1} is predicted, on one side, at 1620 cm^{-1} (solution model) and assigned to the pure C=O asymmetric stretching vibration (Table III). The difference between the observed and calculated wavenumbers (37 cm^{-1}) can be explained by the effect of intra-molecular N-H··· O H-bond as shown in (Supplemental Material S3), noting that the DL-tryptophan molecule in the solid state does not have a similar H-bond [12]. On the other side, the same observed band (1657 cm^{-1}) is predicted at ~1650 cm^{-1} using periodic DFT and assigned to the out-of-plane bending vibration of NH^+_3 group.

The band computed by using the solution phase model and seen in Fig. 4a. at 1620 cm^{-1} has the largest intensity (I_{ir}= 700 Km/mole), which is in general agreement with previous calculations [10]. However, a qualitative comparison of the relative intensities of the observed bands at 1657 and 1579 cm^{-1} with the calculated ones by using both the solid phase and solution phase models shows that the former model is the most suitable for interpreting these two bands.

The major contribution in the IR spectrum is due to the indole ring vibrations which are mixed with certain other vibrations as can be seen in Table III.

4. CONCLUSIONS

In this study, the structural and vibrational properties of zwitterionic DL-tryptophan were investigated using IR spectroscopy and DFT calculations performed using both the solid state and aqueous solution models.

The experimental/theoretical comparison has shown that the structural parameters and vibrational wavenumbers calculated using solid state model yield the best agreement with the experimental results. Also, the effects of the intermolecular interactions on the structural and vibrational properties of the considered compound were revealed. The results of our calculations have shown that only the calculations performed using the solid state model allowed us to attribute the broad-band observed at 2532 cm^{-1} to the N-H stretching mode.

Acknowledgments

The authors acknowledge the Technology Hall of the University of Medea and Laboratory of crystallography of the University of Constantine 1 for the use of the available equipments.

REFERENCES

[1] Boldyreva E., (2008) Crystalline amino acids: a link between chemistry, materials science and biology. *Springer: Dordrecht* 167-192.

[2] Wu G., (2009**)** Amino acids: metabolism, functions, and nutrition. *Amino acids* 37, 1-17.

[3] Lamzin V.S., Dauter Z., Wilson K. S., (1995) How nature deals with stereoisomers. *Current opinion in structural biology* 5(6), 830-836.

[4] Hegstrom R. A., Kondepudi D. K., (1990) The handedness of the universe. *Scientific American* 262(1), 108-115.
[5] Blackmond D. G., (2010) The origin of biological homochirality. *Cold Spring Harb. Perspect. Biol* a002147.
[6] Smith C., (1929**)** The ultra-violet absorption spectra of certain aromatic amino-acids, and of the serum proteins. *Proc. R. Soc. Lond. B* 104, 198-205.
[7] Goodwin T. W., Morton R. A., (1946) The spectrophotometric determination of tyrosine and tryptophan in proteins. *Biochem. J* 40(5-6), 628-632.
[8] Ivanova B. B., (2006) IR-LD spectroscopic characterization of L-Tryptophan containing dipeptides. *Spectroc. Acta A* 64, 931-938.
[9] Çakır S., Biçer E., (2010) Synthesis, spectroscopic and electrochemical characteristics of a novel Schiff-base from saccharin and tryptophan. *J. Iran. Chem. Soc* 7, 394-404.
[10] Cao X., Fischer G., (1999) Infrared spectral, structural, and conformational studies of zwitterionic L-tryptophan. *J. Phys. Chem. A* 103, 9995-10003.
[11] Bakke Ø., Mostad A., (1980) The structure and conformation of tryptophan in the crystal of the pure racemic compound and the hydrogen oxalate. *Acta Chem Scand B* 34, 559-570.
[12] Hübschle C. B., Messerschmidt M., Luger P., (2004) Crystal structure of DL-Tryptophan at 173K. *Cryst. Res. Technol* 39, 274-278.
[13] Görbitz H., Törnroos K. W., Day G. M., (2012) Single-crystal investigation of l-tryptophan with Z′= 16. *Acta Cryst B* 68, 549-557.
[14] Zhou T., Wu Y., Cao J., Zou L., Yuan J., Yao Z., Xu G., (2017) Research on the Terahertz Absorption Spectra of Histidine Enantiomer (L) and its Racemic Compound (DL). *Appl. Spectrosc* 71(2), 194-202.
[15] Minkov V. S., Chesalov Yu. A., Boldyreva E. V., (2010) A study of the temperature effect on the IR spectra of crystalline amino acids, dipeptids, and polyamino acids. VI. L-alanine and dl-alanine. *Journal of Structural Chemistry* 51, 1052-1063.
[16] Jarmelo S., Reva I., Carey P. R., Fausto R., (2007) Infrared and Raman spectroscopic characterization of the hydrogen-bonding network in L-serine crystal. *Vib. Spectrosc* 43(2), 395-404.
[17] Jarmelo S., Reva I., Rozenberg M., Carey P. R., Fausto R., (2006) Low-temperature infrared spectra and hydrogen bonding in polycrystalline DL-serine and deuterated derivatives. *Vib. Spectrosc* 41(1), 73-82.
[18] Gronert S., O'Hair R. A., (1995) Ab initio studies of amino acid conformations. 1. The conformers of alanine, serine, and cysteine. *J. Am. Chem. Soc* 117(7), 2071-2081.
[19] Contreras C. D., Ledesma A. E., Lanús H. E., Zinczuk J., Brandán S. A., (2011) Hydration of l-tyrosine in aqueous medium. An experimental and theoretical study by mixed quantum mechanical/molecular mechanics methods. *Vib. Spectrosc* 57(1), 108-115.
[20] Cao X., Fischer G., (2000) The infrared spectra and molecular structure of zwitterionic L-β-phenylalanine. *J. Mol. Struct* 519(1-3), 153-163.
[21] Cao X., Fischer G., (1999) New infrared spectra and the tautomeric studies of purine and αL-alanine with an innovative sampling technique. *Spectroc. Acta A* 55(11), 2329-2342.
[22] Neese F., (2012) The ORCA program system. *WIREs Comput Mol Sci* 2, 73–78.
[23] Becke A. D., (1993) Density-functional thermochemistry. III. The role of exact exchange. *J. Chem. Phys* 98, 5648- 5652.
[24] Lee C., Yang W., Parr R. G., (1988) Development of the Colle-Salvetti correlation-energy formula into a functional of the electron density. *Phys. Rev B* 37, 785-789.
[25] Schafer A., Horn H., Ahlrichs R., (1992) Fully optimized contracted Gaussian basis sets for atoms Li to Kr. *J. Chem. Phys* 97, 2571-2577.

[26] Weigend F., Ahlrichs R., (2005) Balanced basis sets of split valence, triple zeta valence and quadruple zeta valence quality for H to Rn: Design and assessment of accuracy. *Phys. Chem. Chem. Phys* 7, 3297-3305.

[27] Kossmann S., Neese F., (2010) Efficient structure optimization with second-order many-body perturbation theory: The RIJCOSX-MP2 method. *J. Chem. Theory Comput* 6, 2325–2338.

[28] Izsàk R., Neese F., (2013) Speeding up spin-component-scaled third-order pertubation theory with the chain of spheres approximation: the COSX-SCS-MP3 method. *Molecular Physics* 111, 1190–1195.

[29] Osaki T., Soejima E., (2010) Quadratic scaling functions for obtaining normal vibrational wavenumbers from the B3LYP calculation. *Res. Bull. Fukuoka Inst. Tech 42*(2), 129-134.

[30] Yoshida H., Ehara A., Matsuura H., (2000) Density functional vibrational analysis using wavenumber-linear scale factors.*Chem. Phys. Lett* 325, 477–483.

[31] Perdew J. P., Burke K., Ernzerhof M., (1996) Generalized gradient approximation made simple. *Phys. Rev. Lett* 77, 3865.

[32] Clark S. J., Segall M. D., Pickard C. J., Hasnip P. J., Probert M. I., Refson K., Payne M.C., (2005) First principles methods using CASTEP. *Z. Kristallog* 220, 567-570.

[33] Refson K., Tulip P. R., Clark S. J., (2006) Variational density-functional perturbation theory for dielectrics and lattice dynamics.*Phys Rev B* 73(15), 155114.

[34] Min'kov V. S., Chesalov Y. A., Boldyreva E. V., (2008) Study of the temperature effect on IR spectra of crystalline amino acids, dipeptides, and polyamino acids. IV. L-cysteine and DL-cysteine. *Journal of Structural Chemistry* 49(6), 1022-1034.

[35] Petrosyan A. M., (2007) Vibrational spectra of L-histidine perchlorate and L-histidine tetrafluoroborate.*Vib. Spectrosc* 43(2), 284-289.

[36] Chowdhry B. Z., Dines T. J., Jabeen S., Withnall R., (2008) Vibrational spectra of α-amino acids in the zwitterionic state in aqueous solution and the solid state: DFT calculations and the influence of hydrogen bonding.*J. Phys. Chem. A* 112, 10333-10347.

[37] Pawlukojć A., Hołderna-Natkaniec K., Bator G., Natkaniec I., (2014) INS, IR, RAMAN, 1H NMR and DFT investigations on dynamical properties of l-asparagine. *Vib. Spectrosc* 72, 1-7.

[38] Parker S. F., (2013) Assignment of the vibrational spectrum of L-cysteine. *Chemical Physics* 424, 75-79.

[39] Mostad A. R. V. I. D., Romming C., (1973) Crystal-structure of DL-tyrosin. *Acta Chem. Scand* 27, 401-410.

[40] Frey M. N., Koetzle T. F., Lehmann M. S., Hamilton W. C., (1973) Precision neutron diffraction structure determination of protein and nucleic acid components. X. A comparison between the crystal and molecular structures of L-tyrosine and L-tyrosine hydrochloride. *J. Chem. Phys* 58(6), 2547-2556.

[41] Edington P., Harding M. M., (1974) The crystal structure of DL-histidine. *Acta Cryst B* 30(1), 204-206.

Appendix A. The calculated wavenumbrs in solution phase for the internal modes of DL-tryptophan.

N°	ω_{cal} (cm^{-1})	
	Unscaled wavenumbers	Scaled wavenumbers
1	31	**17**
2	49	**36**
3	54	**41**
4	82	**70**
5	146	**136**
6	209	**200**
7	223	**214**
8	236	**228**
9	260	**252**
10	301	**294**
11	306	**299**
12	382	**376**
13	433	**428**
14	444	**439**
15	469	**464**
16	492	**487**
17	551	**546**
18	593	**588**
19	601	**596**
20	636	**631**
21	663	**658**
22	749	**744**
23	753	**748**
24	767	**762**
25	777	**772**
26	786	**781**
27	829	**823**
28	847	**841**
29	865	**859**
30	890	**883**
31	935	**927**

32	938	**930**
33	946	**938**
34	972	**964**
35	1016	**1007**
36	1029	**1020**
37	1069	**1059**
38	1095	**1084**
39	1107	**1095**
40	1130	**1118**
41	1147	**1134**
42	1174	**1160**
43	1209	**1194**
44	1250	**1234**
45	1276	**1259**
46	1316	**1297**
47	1332	**1313**
48	1346	**1326**
49	1362	**1342**
50	1365	**1344**
51	1385	**1364**
52	1399	**1377**
53	1439	**1415**
54	1449	**1425**
55	1478	**1452**
56	1481	**1455**
57	1520	**1492**
58	1581	**1550**
59	1598	**1566**
60	1607	**1574**
61	1643	**1608**
62	1651	**1616**
63	1655	**1620**
64	3004	**2839**
65	3056	**2884**
66	3129	**2946**

76	3160	**2973**
86	3169	**2981**
69	3176	**2987**
70	3186	**2995**
71	3243	**3044**
72	3260	**3058**
73	3462	**3229**
74	3511	**3270**
75	3636	**3375**

ω_{cal} : calculated wavenumbers in (cm^{-1}).

$$\omega_{Scaled} = -0.000028\ \omega^2_{unscaled} + 1.034\ \omega_{unscaled} - 14.77 \quad (cm^{-1})$$

Appendix B. The calculated wavenumbrs in the solid phase for the optical modes of DL-tryptophan. The 321 optical modes are classified into four subgroups according to the irreducible representation of the factor group of DL-tryptophan.

$\mathbf{a_g}$	$\mathbf{b_g}$	$\mathbf{a_u}$	$\mathbf{b_u}$
3389	3396	3397	3389
3170	3170	3170	3170
3118	3118	3117	3118
3108	3108	3108	3107
3098	3098	3100	3099
3094	3094	3095	3095
3045	3079	3057	3074
3021	3023	3023	3021
3006	3005	3005	3006
2933	2935	2965	2950
2930	2931	2932	2932
2559	2557	2561	2571
1656	1643	1650	1669
1633	1637	1619	1630
1603	1606	1607	1603
1562	1565	1562	1582
1557	1560	1558	1559
1540	1538	1533	1535
1532	1527	1518	1532
1479	1471	1474	1475
1444	1442	1443	1445
1440	1437	1438	1441
1418	1424	1423	1419
1385	1373	1382	1381
1359	1355	1355	1358

1349	1345	1347	1348
1330	1339	1330	1337
1312	1311	1311	1311
1294	1296	1297	1303
1279	1281	1280	1280
1245	1243	1245	1244
1220	1222	1220	1220
1199	1199	1200	1201
1155	1164	1151	1163
1137	1156	1135	1151
1124	1132	1122	1132
1112	1109	1109	1112
1085	1088	1087	1083
1052	1056	1056	1054
1043	1040	1040	1043
1004	1004	1004	1002
970	972	979	976
949	953	954	954
947	950	948	948
906	914	912	919
865	866	864	867
850	852	851	850
839	839	841	834
821	820	819	820
765	762	764	762
757	758	760	755
747	747	749	746
735	746	734	737
732	736	729	729
650	649	652	649
629	623	622	627
596	598	597	599
581	591	588	587
578	579	581	579
538	540	539	539
530	537	535	532
521	526	525	522
461	459	459	460
421	421	425	425
390	395	397	388
360	365	377	381
299	324	303	313
263	274	269	275
258	250	250	249
239	230	231	245

218	218	227	229
177	206	189	166
160	165	164	140
143	141	134	117
115	127	105	89
97	101	98	85
96	95	92	71
73	84	83	61
62	62	48	47
50	52	34	
38	29		

a_u and b_u: the IR active modes.
a_g and b_g : the RAMAN active modes.
The wavenumbers are expressed in (cm^{-1}).